Tungsten Oxide Coatings from the Aerosol-Assisted Chemical Vapor Deposition of $W(OAr)_6$ (Ar = C_6H_5, C_6H_4F-4, $C_6H_3F_2$-3,4); Photocatalytically Active γ-WO_3 Films

Warren B. Cross, Ivan P. Parkin,* and Shane A. O'Neill

Christopher Ingold Laboratories, Department of Chemistry, University College London, 20 Gordon Street, London, WC1H OAJ

Paul A. Williams, Mary F. Mahon, and Kieran C. Molloy*

Department of Chemistry, University of Bath, Claverton Down, Bath, BA2 7AY

Received April 16, 2002. Revised Manuscript Received April 11, 2003

Tungsten hexaaryloxide complexes of formula $W(OAr)_6$ (Ar = C_6H_5, **1**; C_6H_4F-4, **2**; $C_6H_3F_2$-3,4, **3**) have been synthesized by the reaction of $W(O)Cl_4$ and ArOH in 22−28% yield. The complexes were characterized by ^1H, ^{13}C, ^{19}F, and ^{183}W NMR (**1**, $\delta = -474.8$; **2**, $\delta = -416.3$; **3**, $\delta = -446.3$), melting point (**1**, 95 °C; **2**, 101 °C; **3**, 105 °C), IR, microanalysis, and single-crystal X-ray diffraction (octahedral coordination). Aerosol-assisted chemical vapor deposition of $W(OAr)_6$ using acetone and toluene solvents and substrate temperatures from 300 to 500 °C produced blue tungsten oxide films on glass substrates. The films were analyzed by glancing angle powder diffraction and shown to be amorphous at 300 °C, but consisted of crystalline WO_{3-x} at higher deposition temperature. Annealing the films from **1** at 550 °C in air for 30 min produced yellow γ-WO_3 with preferred growth in the [020] direction. Raman analysis of the as-formed films showed WO_{3-x} with evidence for W^V-W^{VI} paired ions. Annealed samples produced Raman patterns for γ-WO_3 (807, 715, 273, and 133 cm^{-1}). The films were adhesive to the substrate, conformal, passed the Scotch tape test, and gave good coverage. Typical growth rates were 20−50 nm min^{-1}. SEM showed uniform films consistent with an island growth mechanism. Energy dispersive analysis confirmed the presence of only tungsten and oxygen. XPS showed that the as-formed films were WO_{3-x} ($x \approx 0.22$) with binding energy shifts for W $4f_{5/2}$ at 37.2 and $4f_{7/2}$ 34.4 eV and for oxygen 1s at 532.6 eV. The as-formed films had an absorption maxima at 320−360 nm (dependent on film thickness) and an onset for absorption at 400 nm. Reflectance/transmission measurements produced interference fringes that enabled a calculation of film thickness. In general the films showed good transmission from 500 to 1000 nm (60%) and some reflectivity (ca. 20%) over the same region. After annealing, the absorption edge was pushed more into the visible and the films showed evidence for some scattering associated with haze. The blue WO_{3-x} films showed negligible photocatalytic activity. The annealed, yellow WO_3 films were active photocatalysts and readily destroyed an overlayer of stearic acid.

Introduction

Tungsten oxide thin films have been extensively investigated in recent years.[1] They show somewhat unique optical properties that can be utilized in different devices such as "smart windows", anti-dazzling mirrors, and information displays.[2] They have also been used in sensor technology for detecting ozone and nitrous oxides.[3] One of the reasons for their widespread application is their ability to undergo reversible oxidation/reduction chemistry. Thin films of amorphous WO_{3-x} on conducting and transparent substrates are blue when a negative potential is applied.[4] They become a very pale yellow (virtually colorless) when the potential is switched to positive values. In gas-sensing applications they function by means of a change in charge carrier density in response to exposure to trace amounts of certain gases.[5]

* Authors to whom correspondence should be addressed. I.P.P.: fax 44-207-679-7463; e-mail i.p.parkin@ucl.ac.uk. K.C.M.: fax 01-225-386231; e-mail: k.c.molloy@bath.ac.uk.

(1) Meda, L.; Brietkopf, R. C.; Haas, T. E.; Kriss, R. U. *Thin Solid Films* **2002**, *402*, 126.

(2) Monk, P. M. S.; Mortimer, R. J.; Rosseinsky, D. R. *Electrochromism: Fundamentals and Applications*; VCH: New York, 1995.

(3) Sberveglieri, G.; Depeto, S.; Groppelli, S.; Nelli, P. *Sens. Actuators, B* **1995**, *26−27*, 89. Dwyer, D. J. *Sens. Actuators, B* **1991**, *5*, 155. Tamaki, J.; Zhang, K.; Fujimora, K.; Akiyama, M.; Harada, T.; Miura, N.; Yamazoe, N. *J. Electrochem. Soc.* **1994**, *141*, 2207.

(4) Granqvist, C. G. *Handbook of Inorganic Electrochromic Materials*; Elsevier: New York, 1995. Brescacin, E.; Basato, M.; Tondello, E. *Chem. Mater.* **1999**, *11*, 314.

10.1021/cm020390j CCC: $25.00
Published on Web 06/17/2003

The optical properties and the phase of tungsten oxide film produced are critically dependent on the deposition method. Tungsten oxide films have been deposited by sol−gel,[6] physical vapor deposition,[7] spray pyrolysis,[8] and chemical vapor deposition. The chemical vapor deposition routes include both single-source and dual-source methods. Chisholm[9] has shown that tungsten(VI) oxo-alkoxides and oxo-alkoxide β-diketonate complexes $[WO(OR)_4]$ and $[WO(OR)_3L]$ (R = Bu^t, Pr^iL = acac) provide good single-source precursors for the low-pressure CVD of blue and yellow tungsten oxide films. Presumably the asymmetric metal coordination environment leads to weaker intermolecular packing and higher volatility. Riaz[10] has shown that W(V) and W(VI) ethoxides can be used in the LPCVD of a range of films from $WO_{3.5}$ to $WO_{2.6}$; the phase formed is largely dependent on the temperature of deposition. Plasma-enhanced CVD of WF_6, H_2, and O_2 has been used to prepare stoichiometric films of WO_3 that show good electrochromic response.[11] Tungsten carbonyl[12] and derivatives of tungsten carbonyls[13] have been utilized for the deposition of tungsten oxide thin films. The films, when doped with lithium or hydrogen, show excellent thermochromic response that is directly related to film density.[14] Tungsten oxide films have also been obtained from the dual-source CVD of $WO(OBu^t)_4$ with water.[15]

Photocatalysis is the term that is used to describe the action of light to promote the destruction of a wide range of organic molecules.[16] The process is not actually a catalysis reaction as such, as the light is consumed. To date only one material has shown widespread potential and application in photocatalysis: titania, TiO_2.[17] Both the anatase and rutile forms of TiO_2 can promote the photodestruction of a wide range of hydrocarbons, phenols, acids, and aldehydes, as well as bacteria and viruses.[18] The field has matured to the position where a range of commercial products have hit the marketplace including bathroom tiles, deodorizing granules, bottle coatings, and self-cleaning glass. Pilkington Glass has commercialized the world's first self-cleaning window glass based on an APCVD TiO_2 process:[19] Pilkington Activ glass. It works in two ways: reduction in contact angle on the glass surface (superhydrophillic effect) encouraging sheetlike formation of rain droplets on the surface, and by photocatalytic destruction of dirt and smears on the window surface. Semiconducting titania coatings on glass function by absorbing the sub-320-nm light that is incident on the surface to promote the formation of an electron and a positive hole.[20] These species can either recombine in the bulk or migrate to the surface where they promote oxidation and reduction chemistry of virtually all organic species. One drawback of titania in this application is that it can absorb only a small fraction of the incident sunlight. A photocatalyst with a wider absorption profile could utilize more of the incident sunlight. Despite some early reports that powdered tungsten oxide can function as a photocatalyst[21] this material to our knowledge has not been reported as such in thin film form. In effect it is a somewhat forgotten material with some potential, particularly as its band edge at ca. 400 nm is significantly advanced from that of titania (320 nm).

In this paper we report the synthesis and characterization of $W(OAr)_6$ (Ar = C_6H_5, C_6H_4F-4, $C_6H_3F_2$-3,4) complexes. These materials have proven suitable for the aerosol-assisted chemical vapor deposition (AACVD) of blue WO_{3-x} films on glass substrates. Notably, the oxidized versions of these films show potential as photocatalysts.

Experimental Section

Aerosol-Assisted Chemical Vapor Deposition Studies. Nitrogen (99.99%) was obtained from BOC and used as supplied. Coatings were obtained on SiCO or SiO_2 coated floatglass. AACVD experiments were conducted on 90 mm × 45 mm × 4 mm pieces of glass using a horizontal-bed cold-wall AACVD reactor. The glass was cleaned prior to use by washing it with petroleum ether (60−80 °C) and 2-propanol and then dried in air. A graphite block containing a Whatman cartridge heater was used to heat the glass substrate. The temperature of the substrate was monitored by a Pt−Rh thermocouple. Measurements indicated that temperature gradients of less than 25 °C at 500 °C were noted across the glass substrates. All gas handling lines were made of glass and were of $^1/_4$ in. internal diameter, except for the inlet to the mixing chamber and the exhaust line from the apparatus which were $^1/_2$ in. i.d. and made of stainless steel (Figure 1). The $W(OAr)_6$ precursor was dissolved in either toluene or acetone solvent and an aerosol was generated at room temperature by use of a PIFCO air humidifier. Nitrogen was passed through the aerosol mist, thus forcing the aerosol droplets encapsulated with precursor into the reactor chamber. The exhaust from the reactor was vented directly into the extraction system of a fume cupboard. The coater chamber was baked out with nitrogen at 150 °C for 30 min before the runs. Deposition experiments were conducted by heating the horizontal-bed reactor to the required temperatures before diverting the nitrogen line through the aerosol and hence to the reactor. Deposition experiments were timed by stopwatch for 30 min. At the end of the deposition the aerosol line was closed and only nitrogen passed over the substrate. The glass

(5) Davazoglou, D.; Georgouleas, K. *J. Electrochem. Soc.* **1998**, *145*, 1346.
(6) Ozer, N. *Thin Solid Films* **1997**, *305*, 80. Wang, J.; Bell, J. M.; Skryabin, I. L. *Sol. Energy Mater. Sol. Cells* **1999**, *56*, 465. Pyper, O.; Schollhorn, R.; Donkers, J. J. T. M.; Krings, L. M. H. *Mater. Res. Bull.* **1998**, *33*, 1095.
(7) Deb, S. K. *Philos. Magn.* **1973**, *27*, 801.
(8) Regragui, M.; Addou, M.; Outzourhit, A.; Bernede, J. C.; El Idrissi, E. L. B.; Benseddik, E.; Kachouane, A. *Thin Solid Films* **2000**, *358*, 40.
(9) Baxter, D. V.; Chisholm, M. H.; Doherty, S.; Gruhn, N. E. *Chem. Commun.* **1996**, 1129.
(10) Riaz, U. *Thin Solid Films* **1993**, *238*, 15.
(11) Henley, W. B.; Sacks, G. J. *J. Electrochem. Soc*, **1997**, *144*, 1045.
(12) Gogova, D.; Gesheva, K.; Kakanakova-Georgieva, A.; Surtchev, M. *Eur. Phys. J.* **2000**, *11*, 167. Davazoglou, D.; Moutsakis, A.; Valamontes, V.; Psycharis, V.; Tsamakis, D. *J. Electrochem. Soc.* **1997**, *144*, 595. Kaplin, L. H.; d'Heurle, F. M. *J. Electrochem. Soc.* **1970**, *117*, 693. Davazogolou, D.; Donnadieu, A. *Thin Solid Films* **1988**, *164*, 369. Maruyama, T.; Kanagawa, T. *J. Electrochem. Soc.* **1994**, *141*, 2435.
(13) Gordon, R. G.; Barry, S.; Barton, J. T.; Broomhall-Dillard, R. N. R. *Thin Solid Films* **2001**, *392*, 231.
(14) Henley, W. B.; Sacks, G. J. *J. Electrochem. Soc.* **1997**, *144*, 1045.
(15) Basato, M.; Brescacin, E.; Tondello, E. *Chem. Vap. Deposition* **2001**, *7*, 219.
(16) Mills, A.; Le Hunte, S.; *J. Photochem. Photobiol.* **1997**, *108*, 1.
(17) Fujishima, A.; Honda, K. *Acc. Chem. Res.* **1995**, *28*, 3.
(18) Maysunaga, T.; Tomoda, R.; Nakajima, T.; Wake, H. *FEMS Microbiol. Lett.* **1985**, *29*, 211.
(19) Pilkington Active Glass; www.pilkington.com.
(20) Schwitzelbel, J.; Ekerdt, J. G.; Gerischer, H.; Heller, A. *J. Phys. Chem.* **1995**, *99*, 5633. Tatsuma, T.; Tachibana, S.; Miwa, T.; Tryk, D. A.; Fujishima, *J. Phys. Chem. B* **1999**, *103*, 726.
(21) Mills, A.; Darwent, J. R. *J. Chem. Soc., Faraday Trans. 2* **1982**, *78*, 359. Barbeni, M.; Pramautro, E.; Pelizzetti, F.; Borgarello, E.; Gratzel, M.; Sepone, S. *Chemosphere* **1985**, *14*, 195.

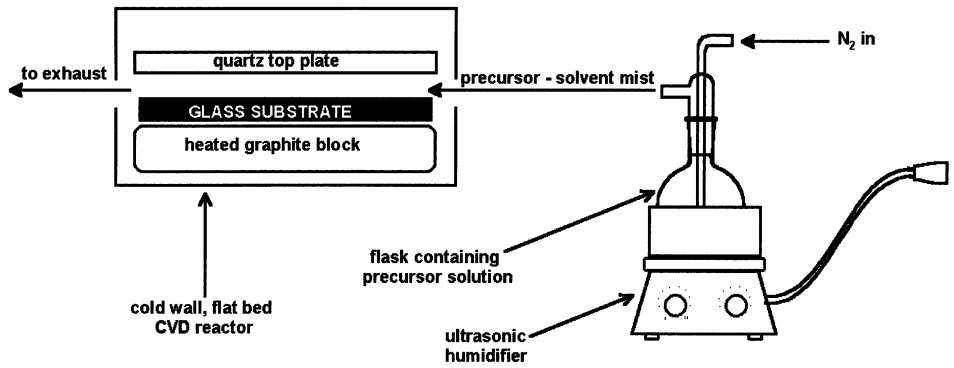

Figure 1. Schematic diagram of the aerosol-assisted chemical vapor deposition reaction setup.

Table 1. Crystallographic Data Collection Parameters

	1	2	3
empirical formula	$C_{36}H_{30}O_6W$	$C_{36}H_{24}F_6O_6W$	$C_{36}H_{18}F_{12}O_6W$
formula weight	742.45	850.40	958.35
temperature, K	293(2)	293(2)	293(2)
wavelength, Å	0.71069	0.70930	0.71069
crystal system	monoclinic	monoclinic	monoclinic
space group	$P2_1/n$	$P2_1/n$	$C2/c$
a, Å	13.702(1)	14.086(3)	20.546(3)
b, Å	16.163(4)	16.863(4)	12.056(2)
c, Å	13.893(1)	14.205(4)	26.991(7)
β, °	90.39(1)	103.37(2)	95.76(2)
volume, Å^3	3076.7(5)	3282.7(14)	6652(2)
Z	4	4	8
density (calc), mg/m^3	1.603	1.721	1.914
reflections collected	4799	5121	3979
reflections $I > 2\sigma(I)$	3122	2723	2165
final R indices [$I > 2\sigma(I)$]	R1 = 0.0392 wR2 = 0.0952	R1 = 0.0580 wR2 = 0.1448	R1 = 0.0801 wR2 = 0.1756

$R = \sum||F_o| - |F_c||/\sum|F_o|$. $R_w = [\sum w||F_o| - |F_c||^2/\sum w|F_o|^2]^{1/2}$.

substrate was allowed to cool with the graphite block to ca. 60 °C before it was removed. Coated substrates were handled and stored in air. The large coated glass sample was broken up into ca. 1 cm × 1 cm squares for subsequent analysis by XPS, EDXA, SEM, electron probe, transmission/reflectance, and UV absorption studies. Large pieces of glass (ca. 4 cm × 4 cm) were used for sheet resistance, X-ray powder diffraction, infrared, contact angle, photocatalysis, and Scotch tape tests. Annealing studies were performed by heating the coated glass sample within the CVD reactor at 550 °C for 30 min under a flow of air.

Film Analysis Methods. X-ray powder diffraction patterns were measured on a Siemans D5000 diffractometer using monochromated CuKα_1 radiation (λ = 1.5406 Å) in the reflection mode using glancing angle incidence (1.5°). Samples were indexed using Unit Cell software and compared to database standards. SEM/EDAX was obtained on a Hitachi S570 instrument using the KEVEX system. Electron microprobe analysis was obtained on a JEOL EMA and referenced against oxygen and titanium standards. X-ray photoelectron spectra were recorded with a VG ESCALAB 220i XL instrument using focused (300 μm spot) monochromatic Al Kα radiation at a pass energy of 20 eV. Scans were acquired with steps of 50 meV. A flood gun was used to control charging, and the binding energies were referenced to an adventitious C 1s peak at 284.8 eV. Depth profile measurements were obtained by using argon beam sputtering. UV−vis spectra were recorded in the range 200−1000 nm using a Helios double-beam instrument. Reflectance and transmission spectra were recorded between 300 and 1100 nm by a Zeiss miniature spectrometer and between 300 and 2600 with a Hitachi UHB instrument. Measurements were standardized relative to a rhodium mirror (reflectance) and air (transmission). Raman spectra were acquired on a Renishaw Raman System 1000 using a helium−neon laser of wavelength 632.8 nm. The Raman system was calibrated against the emission lines of neon. Contact angle measurements of selected glass samples were determined by measuring the spread of a 7.5-μL droplet of water and applying a suitable program. Electrical conductivity was determined by a 4-probe device. Hardness scratch tests were conducted with felt pads, a brass stylus, and a stainless steel scalpel.

Photocatalysis Measurements. Photocatalysis of the samples was assessed by the destruction of an over-layer of stearic acid on a 4 cm × 4 cm portion of glass. The stearic acid was applied by dropping 7.5 μL of 0.4 M stearic acid onto the glass surface. The glass was spun at 3000 revolutions a minute during the dropping procedure. The IR spectra of the stearic acid over-layer was measured over the range 3000−2800 cm^{-1}. The stearic acid coated glass was irradiated at 30-min intervals for up to 2 h with 254-nm radiation provided by BDH germicidal lamps (2 × 8 W).

Synthesis, General Conditions. All manipulations of tungsten oxychloride were carried out under a nitrogen or argon atmosphere using standard Schlenk techniques or in a drybox fitted with a recirculation system. Once the reactions were complete no special handling of the synthesized compounds was required. ^{183}W NMR were referenced relative to 1 mol dm^{-3} Na_2WO_4/D_2O.

*$W(OC_6H_5)_6$ (**1**).* Phenol (38.0 g, 0.410 mol) was added to tungsten oxychloride (13.8 g, 41.0 mmol) in the absence of any solvent. The reaction mixture was then refluxed for 6 h with occasional stirring. The excess phenol was then sublimed from the reaction mix to yield a dark red solid. Extraction with 500 mL of ether gave a dark red solution which was washed with ~5% NaOH solution (3 × 100 mL). The ether was then removed in vacuo to give a red solid. This solid was recrystallized from methanol to yield dark red needle crystals of $W(OC_6H_5)_6$ (**1**) that were suitable for single-crystal X-ray diffraction. Yield: 7.99 g (26%). Melting point: 95 °C. Calculated for $C_{36}H_{30}O_6W$ (%): C, 58.2; H, 4.05. Found: C, 57.9; H, 4.05. ^{183}W NMR [d^8 Toluene]: −474.8, s. δ_H [$CDCl_3$]: 6.86 [18H, m, 18C*H*]; 7.21 [12H, m, 12C*H*]. δ_C [$CDCl_3$]: 120.4 [*C*H]; 123.4 [*C*H]; 128.8 [*C*H]; 161.8 [*C*O]. υ (NaCl plates, Nujol mull/

cm^{-1}): 1583, 1228, 1161, 1068, 877, 860, 752, 686, 646.

*$W(OC_6H_4F\text{-}4)_6$ (**2**).* Tungsten hexa(parafluorophenoxide) was prepared by a method similar to that used for compound **1**. Tungsten oxychloride (2.12 g, 5.85 mmol) and parafluorophenol (6.58 g, 58.5 mmol) were used in the absence of any solvent to give red crystals of the expected product. Yield: 1.41 g (28%). Melting point: 101 °C. Calculated for $C_{36}H_{24}F_6O_6W$ (%): C, 50.8; H, 2.84. Found: C, 50.8; H, 2.84. ^{183}W NMR [d^8 Toluene]: −416.3, s. δ_H [$CDCl_3$]: 6.79 [12H, m, 12C*H*]; 6.91 [12H, m, 12C*H*]. δ_C [$CDCl_3$]: 115.5 [d, *C*H], $^2J_{CF}$ = 24 Hz; 121.2 [d, *C*H], $^3J_{CF}$ = 8 Hz; 157.6 [d, *C*O], $^4J_{CF}$ = 2 Hz; 159.1 [d, *C*F], $^1J_{CF}$ = 243 Hz. δ_F [$CDCl_3$]: −118.8 [m, C*F*]. υ (NaCl plates, Nujol mull, cm^{-1}): 1493, 1246, 1196, 1145, 1087, 879, 831, 796.

*$W(OC_6H_3F_2\text{-}3,4)_6$ (**3**).* Crystals of tungsten hexa(3,4-difluorophenoxide) were synthesized by the same methodology as for compound **1** using 3,4-difluorophenol (8.21 g, 60.9 mmol) and tungsten oxychloride (2.08 g, 6.09 mmol) in the absence of any solvent. Yield: 1.23 g (22%). Melting point: 105−107 °C. Calculated for $C_{36}H_{18}F_{12}O_6W$ (%): C, 45.1; H, 1.89. Found: C, 45.4; H, 2.00. ^{183}W NMR [d^8 Toluene 80 °C]: −446.3, s. δ_H [$CDCl_3$]: 6.58 [6H, m, 6C*H*]; 6.71 [6H, m, 6C*H*]; 7.06 [6H, m, 6C*H*]. δ_C [$CDCl_3$]: 109.5 [d, *C*H], $^2J_{CF}$ = 19 Hz; 115.9 [dd, *C*H], $^3J_{CF}$ = 6 Hz, $^4J_{CF}$ = 3 Hz; 117.1 [d, *C*H], $^2J_{CF}$ = 19 Hz; 147.6 [dd, *C*F], $^1J_{CF}$ = 247 Hz, $^2J_{CF}$ = 14 Hz; 149.8 [dd, *C*F], $^1J_{CF}$ = 251 Hz, $^2J_{CF}$ = 14 Hz; 156.6 [d, *C*O], $^3J_{CF}$ = 9 Hz. δ_F [$CDCl_3$]: −141.6 [m, C*F*]; −134.3 [m, C*F*]. υ (NaCl plates, Nujol mull, cm^{-1}): 1506, 1309, 1248, 1199, 1151, 1103, 966, 810, 721, 667.

X-ray Crystallography. Crystallographic data for **1**−**3** are given in Table 1. For all three samples, data were collected on an Enraf-Nonius CAD-4 four-circle automatic diffractometer and were corrected for Lorentz, polarization, and absorption.[22] For **1** and **2**, all atoms were allowed to vibrate anisotropically and hydrogen atoms were included at calculated positions. In the case of **2**, the larger-than-average crystal used was the second one selected from the sample as measurements on the first, smaller crystal indicated that this material did not diffract strongly at higher Bragg angles.

For **3**, in the final least squares cycles, isotropic restraints were placed on atoms C3, C4, C9, C10, C11, and C17, although all other non-hydrogen atoms were allowed to vibrate anisotropically. Phenyl rings were refined as rigid hexagons. Hydrogen atoms were included at calculated positions where relevant.

In all three cases, structure determination and refinement (full matrix least-squares on F^2) was carried out using SHELX86[23] and SHELX93,[24] respectively; the asymmetric units of the three structures are shown in Figure 2a−c along with the labeling schemes used, and were produced using ORTEX.[25]

Results

Synthesis and Characterization. The tungsten(VI) aryloxide precursors were prepared from reaction of $W(O)Cl_4$ and ArOH (Ar = Ph, **1**; C_6H_4F-4, **2**; $C_6H_3F_2$-3,4, **3**) in the absence of solvent, eq 1.

$$W(O)Cl_4 + 6ArOH \rightarrow W(OR)_6 + 4HCl(g) + H_2O \quad (1)$$

In each case, the product was heated to sublime off the excess phenol, extracted with ether, and washed with sodium hydroxide solution to ensure removal of excess phenol. Extraction with hot methanol produced dark red crystals of **1**−**3** in yields of 22−28%. Despite the increasing peripheral fluorination of the molecules

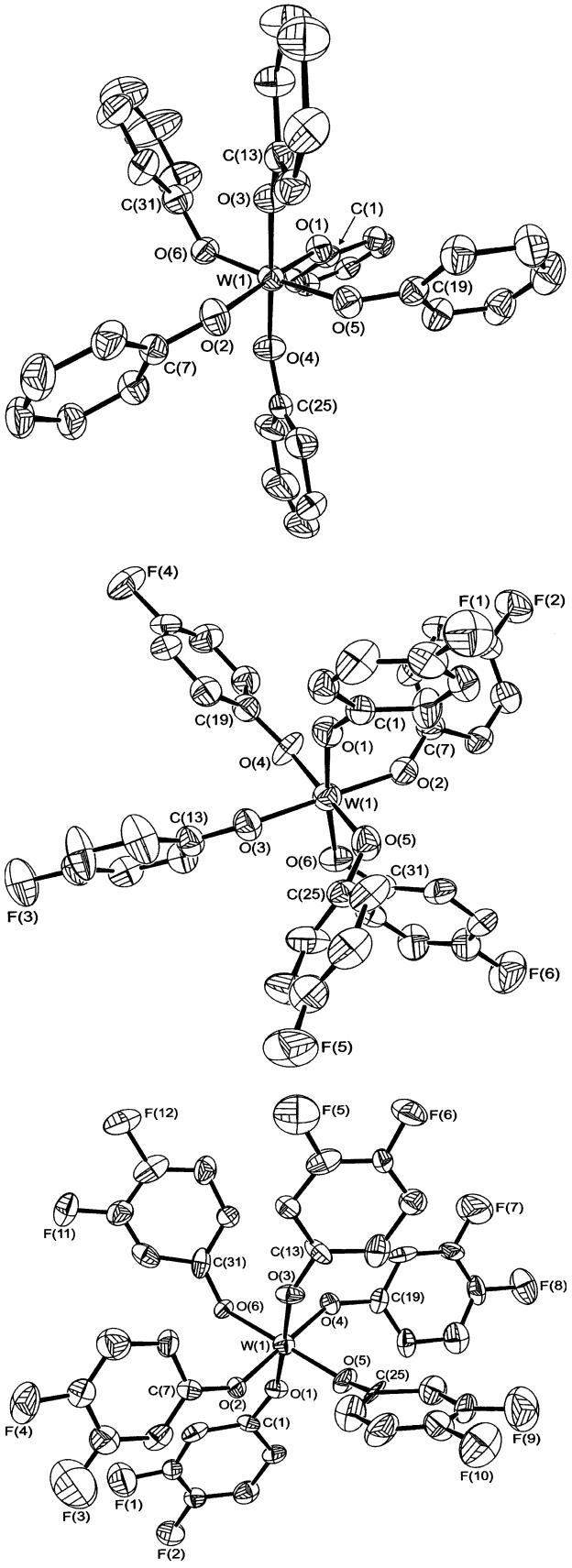

Figure 2. (a) X-ray structure of $W(OPh)_6$ **1** with the atom numbering scheme used in Table 1. Thermal ellipsoids are at the 30% level. (b) X-ray structure of $W(OC_6H_4\text{-}F\text{-}4)_6$ **2** with the atom numbering scheme used in Table 1. Thermal ellipsoids are at the 30% level. (c) X-ray structure of $W(OC_6H_3\text{-}F_2\text{-}3,4)_6$ **3** with the atom numbering scheme used in Table 1. Thermal ellipsoids are at the 30% level.

(22) Walker, N.; Stewart, D. *Acta Crystallogr.* **1983**, *A46*, 158.
(23) Sheldrick, G. M. *SHELX 86S, A Computer Program for Crystal Structure Determination*; University of Gottingen: Gottingen, Germany, 1986.
(24) Sheldrick, G. M. *SHELX 93, A Computer Program for Crystal Structure Refinement*; University of Gottingen: Gottingen, Germany, 1993.
(25) McArdle, P. *J. Appl. Crystallogr.* **1995**, *28*, 65.

Table 2. Summary of Tungsten Oxygen Bond Lengths (Å) and cis O−W−O (°)[a] Angles in 1, 2, 3 and Related Compounds

	1	2	3	$W(OPh)_6$[29]	$W(OC_6H_4Me\text{-}4)_6$	$[W(OPh)_6]^{-}$[b]
W(1)−O(1)	1.896(6)	1.910(8)	1.879(12)	1.883(4)	1.894(4)	n/a
W(1)−O(2)	1.878(7)	1.887(8)	1.896(12)	1.884(4)	1.887(3)	n/a
W(1)−O(3)	1.878(6)	1.871(8)	1.932(11)	1.897(4)	1.896(3)	n/a
W(1)−O(4)	1.874(7)	1.899(8)	1.899(12)	1.908(4)	1.889(3)	1.932(5)
W(1)−O(5)	1.884(6)	1.912(8)	1.882(13)	1.905(4)	1.913(3)	1.956(4)
W(1)−O(6)	1.892(6)	1.916(8)	1.883(13)	1.917(4)	1.891(3)	1.940(5)
mean	1.884(6)	1.899(8)	1.895(12)	1.899(4)	1.895(9)	1.943
O−W−O [a]	88.1(3)	85.7(4)	88.6(6)	87.5(2)	86.1(2)	88.1
	92.9(3)	94.6(4)	92.1(6)	92.6(2)	94.7(1)	91.9

[a] Min, max values. [b] $[Et_4N]^{+}$.

Table 3. Deposition Conditions

precursor	solvent/ concentration gcm^{-3}	reactor temperature °C	flow rate of nitrogen L/min^{-1}	run time minutes	phase seen by XRD	phase seen by Raman
$W(OPh)_6$ (**1**)	toluene 0.01	450	1.2	26	γ−WO_3	
$W(OPh)_6$ (**1**)	acetone 0.02	300	1.0	30	amorphousW	
$W(OPh)_6$ (**1**)	acetone 0.02	400	1.0	30	γ−WO_3	
$W(OPh)_6$ (**1**)	acetone 0.02	500	1.0	30	γ−WO_3	
$W(OC_6H_4F\text{-}4)_6$ (**2**)	toluene 0.01	300	1.0	30	amorphous	
$W(OC_6H_4F\text{-}4)_6$ (**2**)	toluene 0.01	450	1.2	40	γ−WO_3	
$W(OC_6H_3F_2\text{-}3,4)_6$ (**3**)	toluene 0.01	300	1.0	30	amorphous	
$W(OC_6H_3F_2\text{-}3,4)_6$ (**3**)	toluene 0.01	450	1.0	30	γ−WO_3	γ−WO_3

from **1** to **3**, no decrease in melting point (and hence volatility) was achieved; in fact, the melting points increased with increasing relative molecular mass.

The ^{1}H, ^{13}C, and ^{19}F NMR are fully consistent with the hexaaryloxide products. Measurement of the ^{183}W NMR gave a single peak for each compound: **1**, −478.8; **2**, −416.3; **3**, −446.3 ppm. Tungsten has a chemical shift range in excess of 5000 ppm, with the resonance position strongly dependent on the coordination environment.[26] The most highly shielded compound is WF_6 with a chemical shift of −1117 ppm.[27] Although the data are not extensive (^{183}W: $WF_5(OPh)$ −916 ppm; $WO_2(C_5H_{10}NO)_2$ −337 ppm, and $WO(OC_6H_3Pr^{i}_2\text{-}2,6)_4$ −493.6 ppm)[28] the chemical shifts of **1**−**3** mirror other W(VI) species with similar bonding environments.

The crystal structures of **1**−**3** were determined, and are shown in Figure 2. All of the crystals were dark red needles that were stable in air. In each structure the tungsten atom is surrounded by six oxygen atoms from the phenol rings in a slightly distorted octahedral geometry. The crystal structure of **1** has been reported before,[29] however, the refinement had significant disorder. Table 2 shows the tungsten oxygen bond lengths and cis O−W−O bond angles in **1**−**3** compared with those in related compounds.[30] The W−O bond lengths vary between 1.874 and 1.932 Å for all of **1**−**3** with average W−O bond lengths of 1.884(6) Å, **1**; 1.899(8) Å, **2**; and 1.895(12) Å, **3**. These bond lengths are significantly shorter than that found in $[W(OPh)_6]^{-}$ at 1.943 Å[31] but directly comparable to $[W(OC_6H_4Me\text{-}4)_6]$ at 1.895(9) Å[29] and the previously determined structure for $[W(OPh)_6]$ at 1.899(4) Å.[25] The slight deviations from regular octahedral geometry and variation from O−W−O cis angles of 90° is most likely due to changes in packing rather than electronic effects. Molecular orbital calculations on $W(OR)_6$ indicate that an octahedral geometry is favored over trigonal prismatic and D_3 symmetry structures.[33]

Chemical Vapor Deposition Studies. Despite the melting points of **1**−**3** (95, 101, and 105 °C), insufficient carryover was achieved for deposition of films by both single- and dual-source atmospheric-pressure chemical vapor deposition (APCVD). A number of experiments were conducted using low-pressure chemical vapor deposition (LPCVD). These invariably failed, though some significant carryover at a bubbler temperature of 220 °C was noted for **1** at low pressure (10^{-3} atm), associated with sublimation of the precursor. Unfortunately, the precursor recondensed intact on the cold wall of the LPCVD reactor and gave only poor film coverage on the heated substrate. These problems were successfully circumvented using chemical vapor deposition under aerosol-assisted conditions (AACVD). In all cases the AACVD method provided uniform films that covered the whole of the glass substrate. Two solvents were chosen for the APCVD study, encompassing a survey study of all of **1**−**3** in toluene and a detailed investigation of **1** using acetone, Table 3. In all cases the reaction was a single-source process and no oxygen gas or readily available oxygen source (H_2O, ROH) was utilized.

AACVD reactions of **1**−**3** using toluene solvent were studied at substrate deposition temperatures of 300 and 450 °C. At 300 °C deep blue films were formed that covered the whole of the substrate. Some interference fringes were noted. The films were adherent, passing the Scotch tape test. At 450 °C the deposited film consisted of two parts, a well adhered deep-blue film and a powdery black/blue-back surface deposit. The

(26) Minelli, M.; Enemark, J. H.; Brownlee, R. T. C.; O'Connor, M. J.; Wedd, A. J. *Coord. Chem. Rev.* **1985**, *68*, 169.
(27) McFarlane, W.; Noble, A. M.; Winfield, J. M. *J. Chem. Soc. A* **1971**, 948.
(28) McDonell, A. C.; Vasudevan, S. G.; O'Connor, M. J.; Wedd, A. G, *Aust. J. Chem.* **1985**, *38*, 1017.
(29) Struchkov, Yu. T.; Lobanova, G. M. *Chem. Abs.* **1960**, *54*, 8208a. Lehtonen, A.; Sillanpää, R. *Polyhedron* **1998**, *18*, 175.
(30) Clegg, W.; Errington, R. J.; Kraxner, P.; Redshaw, C. *J. Chem. Soc., Dalton Trans.* **1992**, 1431.
(31) Davies, J. I.; Gibson, J. F.; Skapski, A. C.; Wilkinson, G.; Wong, W. *Polyhedron* **1982**, *1*, 641.
(32) Williams, P. A. Ph.D. Thesis, University of Bath, U.K., 1998.
(33) Chisholm, M. H.; Parkin, I. P.; Strieb, W. B.; Eisenstein, O. *Inorg. Chem.* **1994**, *33*, 812.

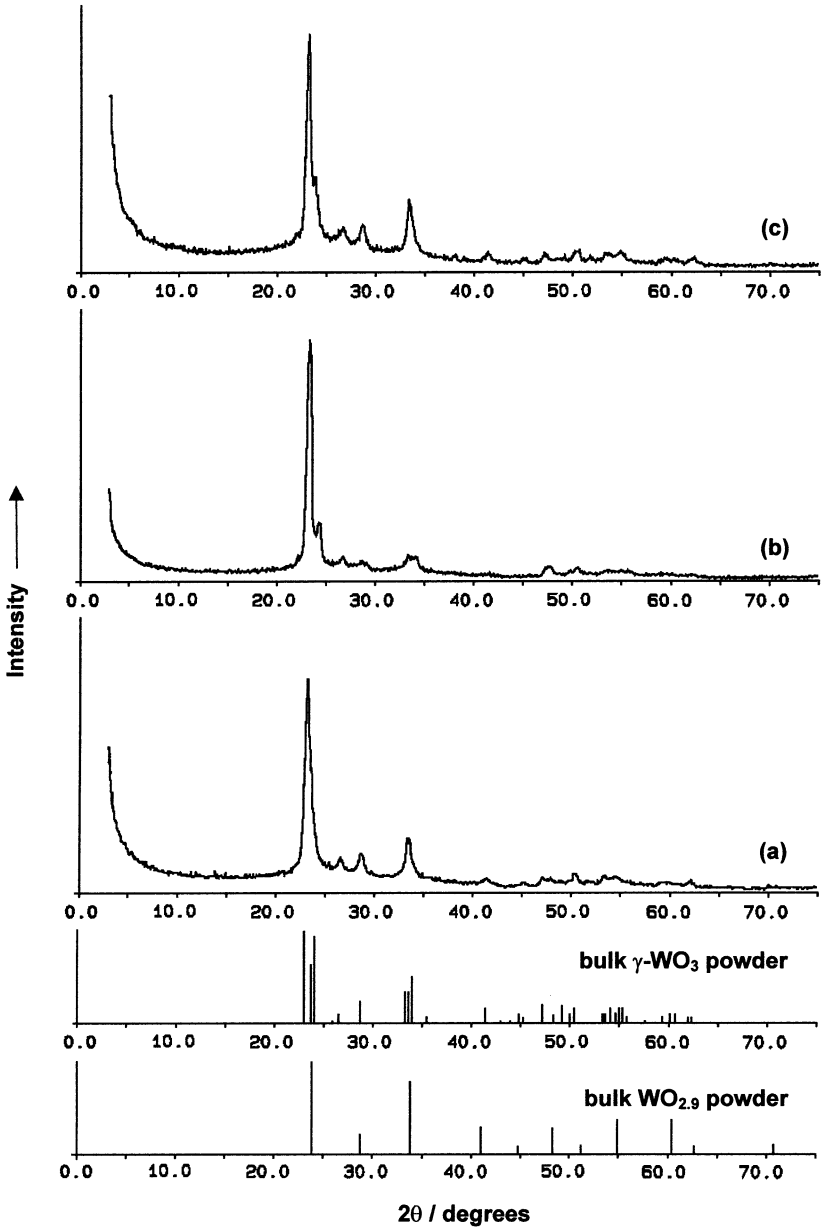

Figure 3. Glancing-angle X-ray diffraction patterns of the films obtained from the AACVD of (a) $W(OPh)_6$ **1**, (b) $W(OC_6H_4\text{-}F\text{-}4)_6$ **2**, (c) $W(OC_6H_3\text{-}F_2\text{-}3,4)_6$ **3** in toluene solvent.

surface deposit was removed by wiping with a soft tissue and was assigned to carbon formed by decomposition of the toluene used to form the aerosol.

The AACVD reaction of **1** using acetone solvent was studied at 300, 400, and 500 °C. The films were blue, well adhered, and fully covered the substrate. No evidence of a powdery overlayer of carbon residue was noted. The blue films did not show any interference fringes. They could not be dislodged by wiping with a soft tissue and passed the Scotch tape test. However, the films formed at 300 and 400 °C could be marked with a brass stylus and stainless steel scalpel.

The blue films showed only minimal change in optical properties after storage in air for up to two years with the edges of the films showing some yellowing. All of the films in this study were analyzed by glancing-angle X-ray diffraction, SEM/EDX, transmission/reflection, and absorption measurements. Selected films from the acetone studies were analyzed in detail by XPS and Raman microscopy.

The X-ray powder diffraction patterns of the films prepared by AACVD using toluene solvent at 300 °C showed only broad amorphous features. Depositions at 450 °C of **1**−**3** all showed similar diffraction patterns consistent with formation of randomly oriented WO_3 (ICDD 20-1324) with a minor amount of $WO_{2.9}$ (ICCD 18-1417)[34] (Figure 3). Some preferred growth was noted in the [001] direction. X-ray analysis of the AACVD (using **1** in acetone) showed an amorphous film at 300 °C and γ-WO_3 at 400 and 500 °C[35] (Figure 4). The γ-WO_3 phase showed striking preferred orientation, with only the 020 and 040 reflections visible. Annealing these samples at 500 °C for 2 h in air induced some crystallinity in the film deposited at 300 °C, giving a pattern for randomly orientated γ-WO_3. Annealing of the films

(34) Zhang, J.; Wessel, S. A.; Collow, K. *Thin Solid Films* **1990**, *185*, 265.

(35) Lee, S. H.; Hyeonsik, M. C.; Liu, P.; Smith, D.; Tracy, C. E.; Mascarenhas, A.; Roland Pitts, J.; Deb, S. K. *Electrochim. Acta.* **2001**, *46*, 1995.

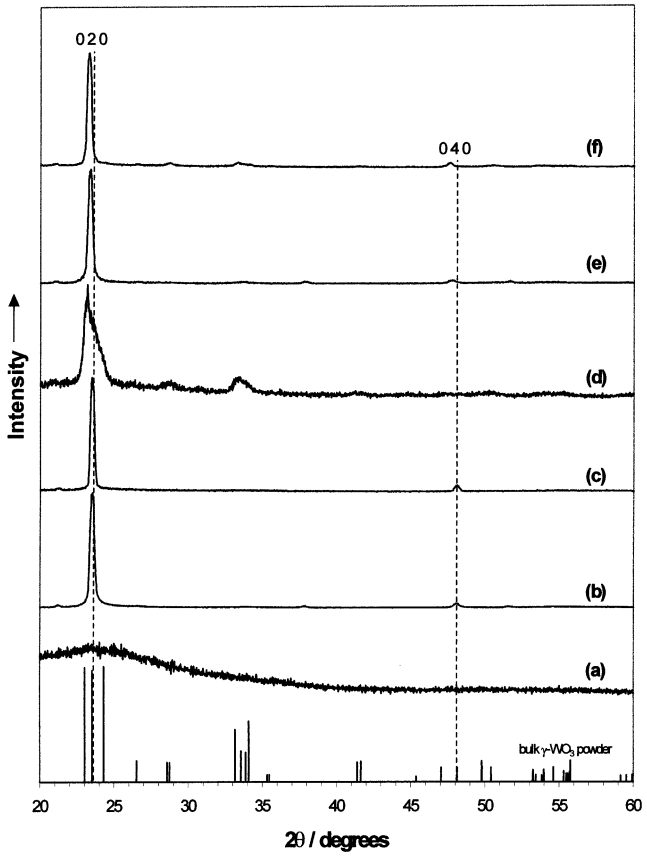

Figure 4. Glancing-angle X-ray diffraction patterns of the films obtained from the AACVD of $W(OPh)_6$ **1** in acetone solvent at (a) 300 °C, (b) 400 °C,and (c) 500 °C. Patterns after annealing these films for 2 h at 500 °C are shown in (d), (e), and (f), respectively.

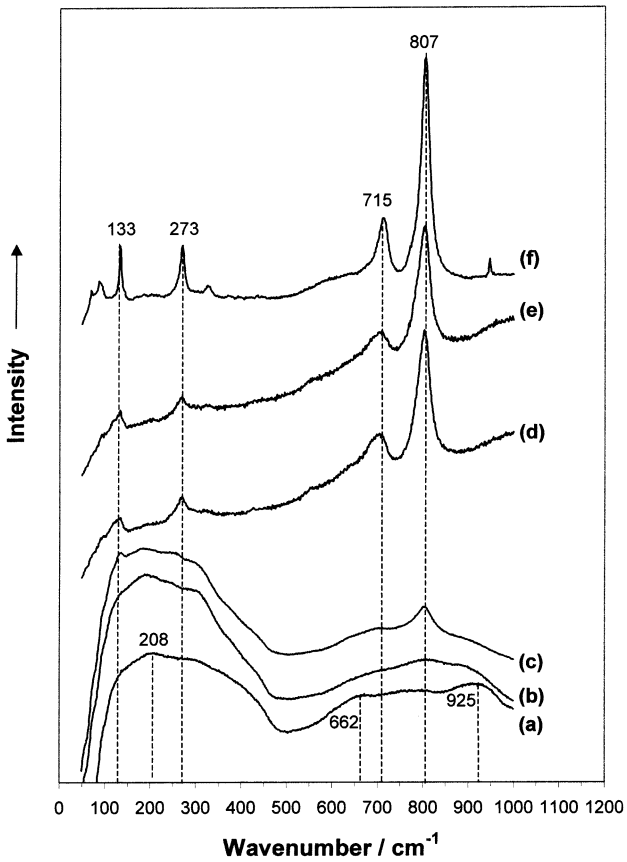

Figure 5. Raman patterns on the films obtained from the AACVD reaction of $W(OPh)_6$ **1** before annealing at substrate temperatures of (a) 300 °C, (b) 400 °C, and (c) 500 °C. Raman patterns of the same films after annealing for 2 h at 500 °C in air are shown in (d), (e), and (f), respectively.

initially produced at 400 and 500 °C gave little real change in the diffraction pattern, although it was noted that the 020 and 040 reflections shifted slightly to lower 2θ, this corresponds to a slightly larger cell and points to higher oxygen content. X-ray line broadening studies on the 020 reflection showed that the as-formed films at 400 °C and above had crystallite sizes in the region of 10−50 nm. This was slightly increased on sintering to ca. 20−60 nm.

Raman patterns were obtained for the films produced by AACVD using **1**/acetone, both before and after annealing at 500 °C for 30 min (Figure 5). Prior to annealing, the Raman patterns were typical of amorphous WO_3 [36] with very broad bands at 925, 760, 662, 320, 208, and 133 cm^{-1}. The band at 208 cm^{-1} is indicative of a partially reduced tungsten species and has been assigned to a W^V-O-W^{VI} bending mode.[37] The bands at 320 and 138 cm^{-1} have been assigned to a W−O−W bending mode for W^{VI} and the higher frequency bands at 662 and 760 cm^{-1} were assigned to the associated W−O−W stretching modes. The highest frequency band is due to a W═O stretch. Notably the Raman patterns obtained from **1** at 400 and 500 °C show sharper features, a loss of the band at 208 cm^{-1}, and growth of bands at 807, 715, and 133 cm^{-1}. These latter bands can be directly assigned to monoclinic γ-WO_3.[38] Annealing the samples in air had a profound change to the Raman bands. All of the annealed films gave patterns for monoclinic γ-WO_3.[39] Notably the Raman bands were more well defined for the film that had been laid down at the highest substrate temperature. The bands seen at 273 and 332 cm^{-1} correspond to the W−O−W bending modes of the bridging oxygen, and the bands at 715 and 807 cm^{-1} correspond to the associated stretching modes.[38] A weak Raman band was noted at 945 cm^{-1} for the film formed at 500 °C after annealing, this is probably due to a W═O stretch.[35] The films produced by AACVD in toluene were also assessed prior to annealing. These showed Raman bands due to WO_{3-x}.

Scanning electron microscopy showed that the films grew with an island growth mechanism. Images obtained from tilt photographs enabled ready identification of the glass, undercoated SiCO layer, and crystalline tungsten oxide film (Figure 6). The SEM images showed that the coatings laid down at 300 and 400 °C had some scratch marks on the surface, probably caused by handling, whereas the films deposited at 450 and 500 °C showed none of these marks. The SEM images also showed that the surface had some associated roughness and that some large island growths protrude above the

(36) Wijs, G. A.; de Groot, R. A. *Electrochim. Acta* **2001**, *46*, 1989.
(37) Ramans, G. M.; Garbusenok, S.; Veispals, A. A. *Phys. Stat. Sol.* **1982**, *74*, K41.
(38) Santato, C.; Odziemkowski, M.; Ulmann, M.; Augustynski, J. *J. Am. Chem. Soc.* **2001**, *123*, 10639.
(39) Gogova, G.; Gesheva, K.; Kakanakova-Georgieva, A.; Surtchev, M. *Eur. J. Phys.* **2000**, *11*, 167.

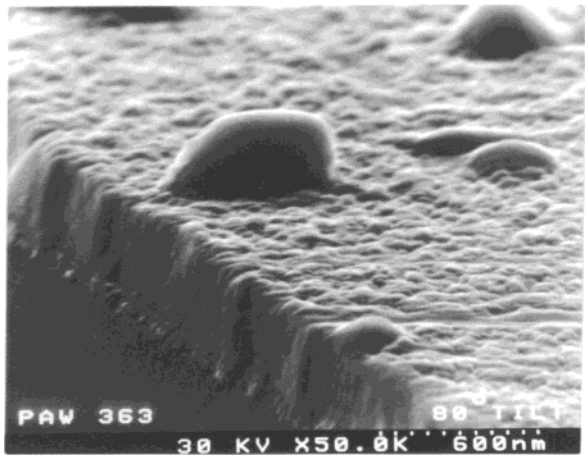

Figure 6. Scanning electron microscope 80° tilt photograph of the film prepared from the AACVD of **2** at 450 °C.

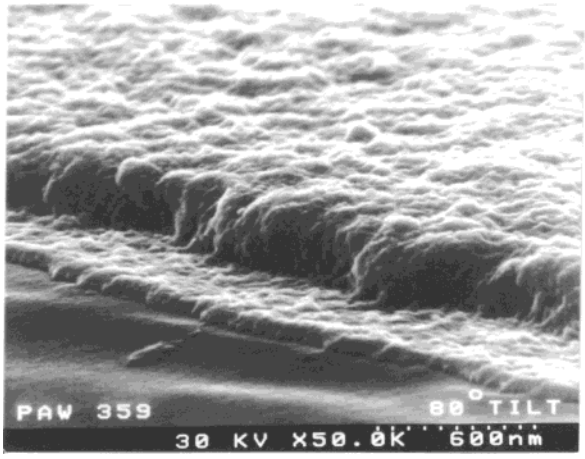

Figure 7. Scanning electron microscope 80° tilt photograph of the film prepared from the AACVD of **1** at 450 °C.

average plane of the film (Figure 7). Film thicknesses were determined from the SEM measurements as 230−350 nm, dependent on sample. This gives typical growth rates of 10−15 nm min^{-1}.

Energy dispersive analysis by X-rays (EDAX) showed the presence of only tungsten and oxygen in the films in the expected ratios WO_3 for the yellow films and WO_3−$WO_{2.9}$ for the blue films. Although EDAX has relatively low sensitivity for oxygen determinations the blue films gave consistently higher W to O ratios than the corresponding yellow films.

X-ray photoelectron spectra of the blue films confirmed that the as-formed layers were WO_{3-x} ($x = 0.22$) with binding energy shifts for W $4f_{5/2}$ at 37.2 and W $4f_{7/2}$ at 34.4 eV and for oxygen 1s at 532.6 eV. No carbon was detected in the film by XPS (less that 0.2 at. %). Depth profile analysis by argon sputtering of the film showed that the surface was fully oxidized and that lower layers of the film had multiple environments for tungsten indicating the formation of W° environments. It was not possible to fully discern whether the reduced W environments were caused by preferential sputtering due to the analysis. The binding energy shifts for the W 4f peaks are directly comparable with those of previous studies.[40,41] On surface profiling additional W 4f peaks at 31.6 and 33.2 eV are observed due to reduced W species.[42]

Optical transmission/reflection and absorption measurements were obtained for all of the films. Films prepared by AACVD using toluene solvent for **1**−**3** showed the same optical profile (Figure 8). The films were highly absorbing at 350 nm and from 600 to 1500 nm. The reflectance profile showed a slightly undulating pattern due to interference fringes (peaks at 600 and 1450 nm). The seemingly fine detail in the reflectance, absorption, and transmission profiles at ca. 950 nm is due to noise generated in the detector system − as such noise is seen for many other unrelated samples. However, the tungsten oxide material was more reflective in the infrared region (780−2600 nm) and less so in the visible region (350−780 nm). Films showed maximum transmission in the visible region. Although not ideal, these data point to the fact that WO_3 films have some limited potential as solar control coatings, in that they have highest reflectance in the IR region and good transmission in the visible. Films prepared by the AACVD using **1** in acetone showed optical properties similar to those made in toluene (Figure 9). The films were, however, thicker and showed more interference patterns in the transmission and reflectance spectra. These were sufficient to determine the thickness measurements of the tungsten oxide films using the method of Swanepoel.[39] These gave 200 nm at 300 °C, 510 nm at 400 °C, and 660 nm at 500 °C. These values correlated well with the SEM measurements. After annealing these films in air they had similar visible optical profiles. The absorption maxima was shifted slightly on annealing from 330 to 340 nm, the band edge was also shifted slightly toward the visible part of the spectra. The most striking change on annealing is that the films lose their blue coloration and become pale yellow.

Contact angle measurements for these films before annealing were in the range 48−60°. After annealing and transformation from blue WO_3 to yellow WO_3 these dropped to 5−21°. Lower contact angle measurements were correlated with the thicker samples.

Photocatalysis Measurements. The blue films produced from the AACVD experiments showed negligible destruction of overlayers of stearic acid under illumination with 254 and 365 nm radiation. The destruction of stearic acid was quantified from the reduction in intensity of the C−H stretch at 3000−2800 cm^{-1}. Samples of uncoated glass and blue WO_3 films showed equivalent negligible loss of stearic acid under 254 nm irradiation (ca. 2−3% after 2 h of illumination). Annealed yellow samples of WO_3 were shown to be effective photocatalysts for the destruction of stearic acid under equivalent conditions. The thickest films showed the greatest photocatalytic response. The film that was produced at 500 °C from **1** in acetone after sintering showed 60% destruction of stearic acid after 120 min of irradiation at 254 nm (Figure 10). Notably, the film prepared at 300 °C showed 30% destruction of stearic acid after annealing for 30 min in air, but 50% destruc-

(40) Granquist C. G. *Handbook of Inorganic Electrochemical Materials*; Elsevier: Amsterdam, The Netherlands, 1995.

(41) Henly, W. B.; Sacks, G. J. *J. Electrochem. Soc.* **1997**, *144*, 1045.

(42) Santucci, S.; Lozzi, L.; Maccallini, E.; Passacantrado, M.; Ottavianna, L. *J. Vac. Sci. Technol., A* **2001**, *19*, 1467.

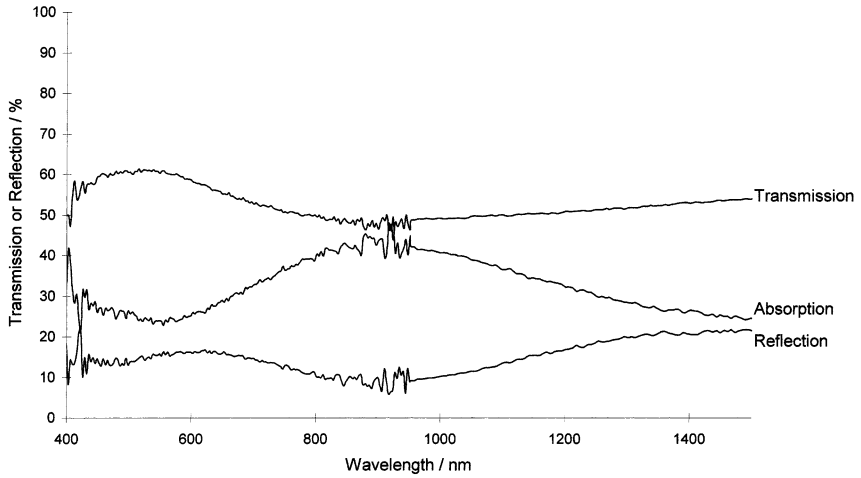

Figure 8. Transmission and reflection plots for the AACVD of **1** in toluene at 450 °C.

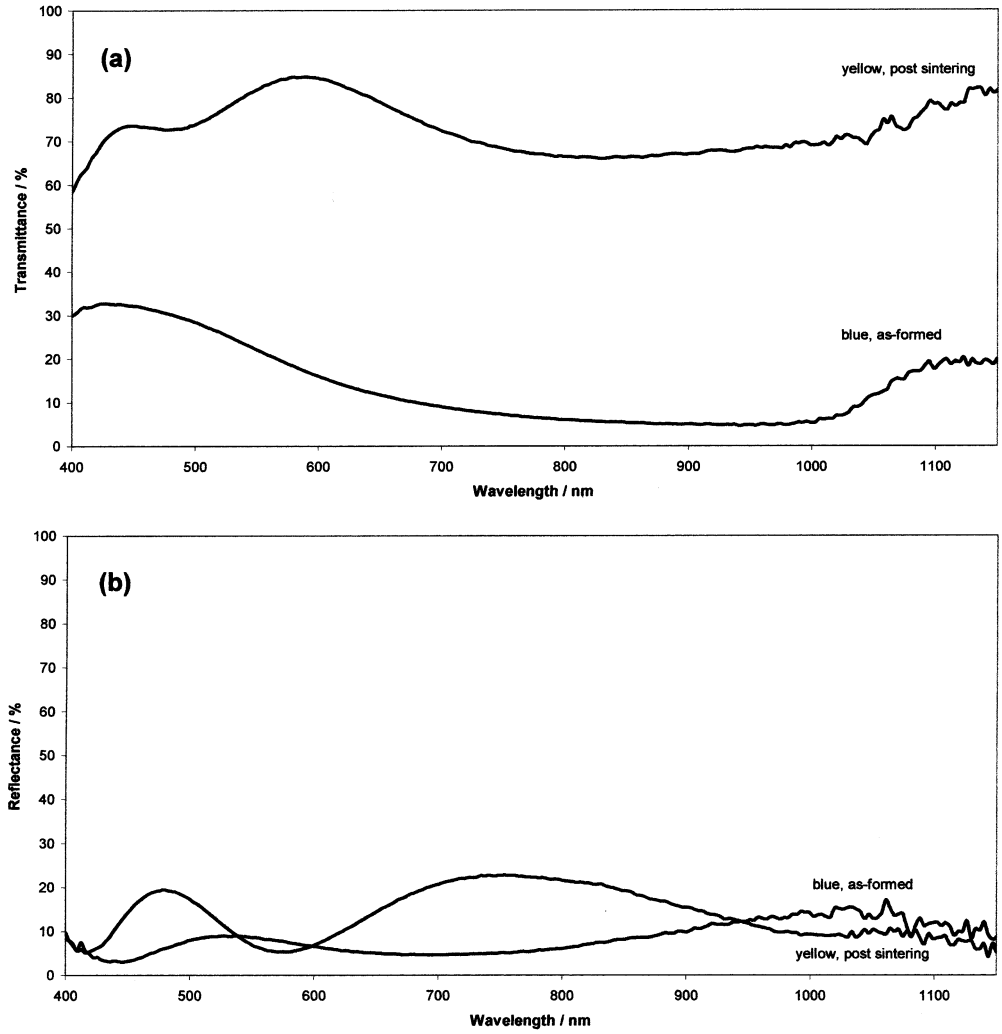

Figure 9. (a) Transmission and reflection plots of **1** in toluene at 450 °C. (b) Reflection plots of the AACVD of **1** in acetone at 400 °C.

tion if the annealing time was extended to 120 min. These results indicate that the photocatalytic activity of the tungsten oxide films is reduced by the presence of reduced forms of tungsten in the films (W^{V}). However in the fully oxidized yellow form they are effective photocatalysts. Indeed, the reactivity of these films at 254 nm is comparable to that of TiO_2 films prepared by APCVD.[43,44]

Further experiments with 365 nm illumination showed a 47% decrease in stearic acid concentration over 24 h for the annealed film from **1**. Although this photoactivity is significantly less than that observed with 254 nm radiation it indicates that the yellow WO_3 films are

(43) Swanepoel, R. *J. Phys. E. Sci. Instrum.* **1983**, *16*, 1214.
(44) Mills, A.; Le Hunte, S. *J. Photochem. Photobiol., A Chem.* **1997**, *108*, 1.

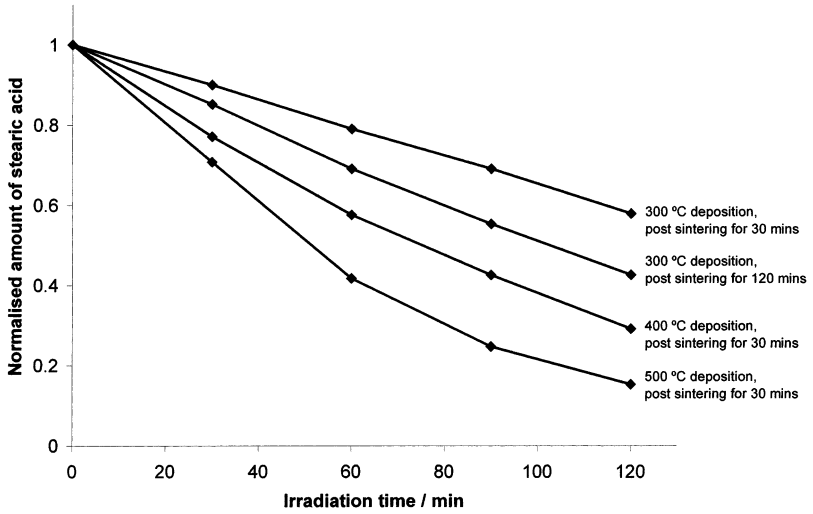

Figure 10. Stearic acid photocatalysis measurements. Plots of percentage stearic acid left on the surface of the glass after irradiation with 254 nm radiation against time.

effective photocatalysts with longer wavelength radiation.

Discussion

$W(OAr)_6$ precursors are easily prepared from commercially available $W(O)Cl_4$, are easy to handle, and are stable in air. The yields obtained in the reactions were low but comparable to those reported for $W(OPh)_6$ prepared from reaction of WCl_6 or $W(NMe_2)_6$ with PhOH[45] and reaction of phenylacetate with tungsten tris(ethylene glycolate)[46] (typically 16−25% yield). Although their volatility is poor (despite melting at ca. 100 °C), their solubility in common organic solvents makes them attractive precursors for AACVD. All of the film analyses indicate that the as-formed films from the AACVD experiments are nonstoichiometric, i.e., partially reduced, WO_{3-x}. The XPS indicates that the films may contain some W(0) species, whereas the XRD and Raman analysis indicate the presence of W(V) oxide in combination with W(VI) oxide. The XPS measurements were on sputtered samples where preferred sputtering is a common phenomena in depth profiling, and in this case ready oxygen loss could be the reason W(0) is observed. The presence of the blue coloration of the films is very indicative of the presence of W(V). Optical properties of the films show that, apart from the aesthetically appealing blue color, the films show some reflectivity in the near-IR and reasonable transmission in the visible. Such a combination of properties is desired in heat-mirror coatings − although detailed studies with thermal infrared would be required to fully explore their potential. These heat-mirror coatings function in windows by allowing visible sunlight through, for example into a room. However, they are reflective in the IR and hence reflect back into a room radiated blackbody energy. Commercial heat-mirror coatings include F-doped SnO_2, Sn-doped indiuim oxide, and titanium nitride coatings. Although showing some useful heat-mirror properties, the blue tungsten oxide coatings are a long way from those currently commercially marketed.

It is not surprising that the CVD initially makes substoichometric films. If the process is assumed to be a single source one then a balanced equation making WO_3 requires elimination of 3 mol of Ar−O−Ar.

Extreme preferred orientation was observed in the XRD for the tungsten oxide coatings formed from acetone AACVD. This was not seen to such a great extent in the XRD of the materials formed from toluene AACVD. One reason for this preferred orientation could be the substrate surface. In the acetone experiments SiO_2 coated glass was used for the depositions, whereas for the toluene experiments SiCO coated glass was used.

The yellow tungsten oxide films show potential as self-cleaning coatings in that they show good photoactivity and a reduction in contact angle to water. Compared to titanium dioxide thin films, the tungsten oxide films show fairly similar photoactivity and contact angle response.[44]

Conclusion

Tungsten aryloxide compounds $W(OAr)_6$ can be readily synthesized by reaction of $W(O)Cl_4$ and the corresponding phenol in moderate yield. The compounds adopted a slightly distorted octahedral geometry. The complexes are not suitable for APCVD or LPCVD as they tend to condense in the carry-gas lines or cold regions of the substrate, however these complexes are eminently suitable for AACVD. Sub-stoichiometric blue films of reduced tungsten oxide WO_{3-x} are obtained from AACVD in both acetone and toluene. Films produced at substrate temperatures below 400 °C are X-ray amorphous and give Raman patterns associated with amorphous WO_{3-x}. Films grown at 450 °C and above were crystalline. The blue tungsten oxide films show some properties associated with a heat mirror, in that they were reflective in the IR and had reasonable transmission in the visible. The blue tungsten oxide films were readily oxidized by heating in air for 30 min to form yellow γ-WO_3. This material showed preferred orientation when deposited on SiO_2 undercoated glass in the [020] direction. The yellow tungsten oxide films are active photocatalysts, readily destroying an overlayer of stearic acid when illuminated with 254 and 365 nm radiation.

(45) Beshouri, S. M.; Rothwell, I. P. *Inorg. Chem.* **1986**, *25*, 1962. Mortimer, P. I.; Strong, M. I. *Aust. J. Chem.* **1965**, *18*, 1579.
(46) Lehtonen, A.; Sillanpää, R. *Polyhedron* **1998**, *18*, 175.

The degree of photoactivity is related to film thickness. The yellow tungsten oxide films also show reduced contact angles. This combination of photoactivity and reduction in contact angle measurement indicate that tungsten oxide films have potential as self-cleaning coatings.

Acknowledgment. I.P.P. and K.C.M. thank the EPSRC and Pilkington Glass for CASE awards to W.B.C. and P.A.W. Dr. D. Sheel and Dr. K. Sandersen of Pilkington glass are thanked for provision of substrates and for useful discussion. I.P.P. and S.O.N. thank the EPSRC for grants GR/M95059 and GR/M82592.

Supporting Information Available: X-ray crystallographic files, in CIF format, for compounds **1**, **2**, and **3** are available free of charge via the Internet at http://pubs.acs.org.

CM020390J